Steel and Composite Structures, *Vol. 21, No. 1 (2016) 37-55*
DOI: http://dx.doi.org/10.12989/scs.2016.21.1.037

Vibration and buckling analyses of laminated panels with and without cutouts under compressive and tensile edge loads

T. Rajanna [*1,2], Sauvik Banerjee [1a], Yogesh M. Desai [1b] and D.L. Prabhakara [3c]

[1] *Department of Civil Engineering, Indian Institute of Technology Bombay, Mumbai 400 076, India*
[2] *Department of Civil Engineering, B.M.S College of Engineering (Autonomous College under VTU), Bengaluru-560019, India*
[3] *Sahyadri College of Engineering & Management, Mangalore 575 007, India*

(*Received July 20, 2015, Revised February 05, 2016, Accepted February 29, 2016*)

Abstract. In this study, the influence of centrally placed circular and square cutouts on vibration and buckling characteristics of different ply-oriented laminated panels under the action of compressive and/or tensile types of non-uniform in-plane edge loads are investigated. The panels are inspected under the action of uniaxial compression, uniaxial tension and biaxial, compression-tension, loading configurations. Furthermore, the effects of different degrees of edge restraints and panel aspect ratios are also addressed in this work. Towards this, a nine-node heterosis plate element has been adopted which includes the effect of shear deformation and rotary inertia. According to the results, the tensile buckling loads are higher than that of compressive buckling loads. However, the tensile buckling load continuously reduces with the increased cutout sizes irrespective of ply-orientations. This is also true for compressive buckling loads except for some particular ply-orientations with higher sized cutouts.

Keywords: laminates; cutout parameters; finite element method; heterosis element; vibration; buckling

1. Introduction

Composite laminates are ideally suited for structural applications of aircraft, spacecraft, mechanical and civil engineering structural components due to their high stiffness to weight ratio and flexibility in design. These laminates have been extensively used in weight sensitive aircraft and aerospace industries since their inception, and recently in civil engineering structures such as bridge decks, bridge girders, strengthening and retrofitting of existing structures. The practical application and complex usability of such materials demand a better understanding of their structural response under various complicated loading conditions. This is particularly true for vibration and buckling response, as the presence of in-plane load alters the free vibration response of structural components. In fact, a situation may encounter that the natural frequency of the structural component becomes zero for a particular intensity of in-plane load and resulting in instability of the components. Hence, the problem of elastic instability is of considerable

*Corresponding author, Ph.D. Scholar, Assistant Professor, E-mail: t.rajanna@gmail.com
[a] Associate Professor, Ph.D., E-mail: sauvik@civil.iitb.ac.in
[b] Professor, Ph.D., E-mail: desai@civil.iitb.ac.in
[c] Director, Ph.D., E-mail: cacep2001@yahoo.com

Copyright © 2016 Techno-Press, Ltd.
http://www.techno-press.org/?journal=scs&subpage=6 ISSN: 1229-9367 (Print), 1598-6233 (Online)

importance and has been the subject of interest to researchers for many years.

Many researchers have investigated the buckling and/or vibration behaviour of panels under uniform edge compression (Afsharmanesh *et al*. 2014, Altunsaray and Bayer 2014, Ashour 2003, Kutlu 2011, Reddy and Phan 1985, Walker 1998). Practically, the in-plane edge loads are non-uniform in nature for many situations. For example, laminated panels are part of a complex structure, and are generally comprised of several interconnected components. The in-plane edge loads transferred to these panels from the connected components can be non-uniform in nature. A limited number of researchers have worked on vibration and/or stability problems of panels under non-uniform edge compression (Lal and Saini 2013, Srivastava *et al*. 2003, Tang and Wang 2011, Zhong and Gu 2007).

Furthermore, cutouts are often used in the design of composite structures for easy access, inspection as well as to pass hydraulic lines, fuel lines and electric lines, and also to reduce the overall weight of the structures (Soni *et al*. 2013). In many cases, the vibration and buckling responses of such perforated structural components are vulnerable in nature. Therefore, in order to prevent premature failure and to utilise their full strength, a complete understanding of the stability behaviour of such panels under the action of non-uniform edge loads is essential.

Yazici *et al*. (2003) carried out an experimental investigation of the effect of U-shaped cutout on stability characteristics of Ly5082 epoxy resin and E-Glass fibre composite plate under the application of uniform in-plane edge loads. Baba (2007), as well as Baba and Baltaci (2007)have also carried out experimental and numerical investigations by using Finite element (FE) package (ANSYS) to study the influence of circular and semi-circular cutouts on stability characteristics of E/glass-epoxy composite panels under uniform edge loads. Topal and Uzman (2008)worked on the optimum design of laminated plate with and without central cutouts under the application of uniform biaxial edge compression using FE method through feasible direction technique. Aydin Komur and Sonmez (2008) carried out the numerical analysis by using FE package (ANSYS) to study the buckling characteristics of isotropic panel by varying the position of circular cutouts along the principal x-axis under the action of uniformly varying loads. The buckling and post-buckling characteristics of different shaped cutout laminated composites under the application of uniform edge loads with different boundary conditions were studied by Kumar and Singh (2010) by using FE formulation. Komur *et al*. (2010) investigated the effects of different layups with circular/elliptical cutout on buckling behaviour of the woven-glass-polyester composite plate under the application of uniform edge compression using FE technique. Singh *et al*. (2012) analysed the buckling characteristics of isotropic plate with cutout by adopting FE package–ANSYS. In their study, they have shown that the plate under partial edge load from both edges exhibiting more buckling resistance as compared to that of plate under central partial edge load. Soni *et al*. (2013) investigated the buckling behaviour of simply supported composite laminates with circular/square cutout subjected to uniaxial non-uniform edge loads using FE package–ABAQUS. Narayana *et al*. (2014) used FE package–ANSYS to investigate the effect of square/rectangular cutout on stability characteristics of quasi-isotropic composite laminates under linearly varying uniaxial edge compression. Recently, Komur and Sonmez (2015) also used FE package–ANSYS to investigate the effects of different uniaxial partial edge load and central circular cutouts on buckling behaviour of isotropic simply supported plates.

The problems considered so far were concerned with compressive edge loading conditions. However, in the majority of cases, panels with/without cutouts are also subjected to the tensile type of non-uniform edge loads. For instance, during the take-off of an aircraft, the lifting force tries to bend the wings upward. Due to this, many upper wing panels are under the application of

non-uniform in-plane edge compression. Similarly, lower wing panels are under non-uniform in-plane edge tension. Usually, no special attention is given to the buckling of such panels when they are subjected to the tensile type of edge loads. These tensile buckling phenomena are practically more important when the panels have defects like crack or cutouts. It may be noted that for a panel with cutout under the action of tensile edge load, the compressive stresses are induced within the vicinity of cutout region. These compressive stresses may result in local tensile buckling, thereby exhibiting complex wrinkles in the zone of compression, which has not received much attention in the past. Leissa and Ayoub (1988) studied the buckling behaviour of isotropic plates under a pair of tensile concentrated forces acting opposite to each other. The vibration and buckling phenomena of isotropic plate subjected to localised tensile patch load and concentrated loads have been studied by Deolasi *et al*. (1995). Kumar *et al*. (2003) have published some results on tensile buckling and vibration behaviour of laminated composite plates and shells subjected to localised patch and concentrated loads. Kumar *et al*. (2002) have investigated the vibration and buckling characteristics of isotropic plate with cutout under the action of partial in-plane edge loads by using FE approach. Shimizu (2007) used FE method to study the effect of different shaped cutouts on tensile buckling behaviour of simply supported isotropic plate. Kremer and Schürmann (2008) studied the influence of shape optimised cutout on tensile buckling behaviour of simply supported square plates using FE approach. In their study, the classical laminate theory is utilised to obtain layer-wise stresses.

Review of the literature reveals that sufficient information is available on vibration and buckling problems of panels under the action of uniformly distributed edge loads. On the contrary, a very limited number of studies deal with the buckling of laminated panels under the action of non-uniform edge compression. Also, there is a paucity of research in the current literature involving tension buckling of laminated panels subjected to non-uniform tensile edge loading. To the best of the authors' knowledge, there is no study involving compression and tension buckling of laminated panels with circular and square cutouts under the action of non-uniform compressive and tensile edge loading.

In the present study, effect of tension and compression buckling of laminated panels with circular and square cutouts are investigated with the influences of various parameters like cutout sizes, boundary conditions, ply-orientations, panel aspect ratios and different type of non-uniform in-plane edge loads.

2. Theory and formulation

A laminated composite panel with a central circular cutout of diameter ϕ, panel length a, breadth b, and thickness h along x-, y- and z-axes respectively is shown in Fig. 1(a). The FE mesh pattern for centrally placed circular and square cutout panels under a typical uniaxial load ($\alpha = 0.5$) along the x-axis is shown in Fig. 1(b) and Fig. 1(c) respectively. The detailed mesh pattern over a quarter panel of circular and square cutout is shown in Fig. 1(d) and Fig. 1(e) respectively. In the analysis, a finer mesh is adopted in the vicinity of cutout, and coarser mesh away from the cutout region. The mesh details are discussed in subsequent convergence studies under the Section 3.1.

Here, P_x^0 is the loading function along the x-axis; P_0 is the loading intensity and α is the load defining factor. By changing the value of load defining parameter α, one can obtain different loading conditions. For instance, $\alpha = 0$ defines uniformly distributed load. On the other hand, $\alpha = 2$ defines the pure in-plane bending as can be seen in Fig. 2.

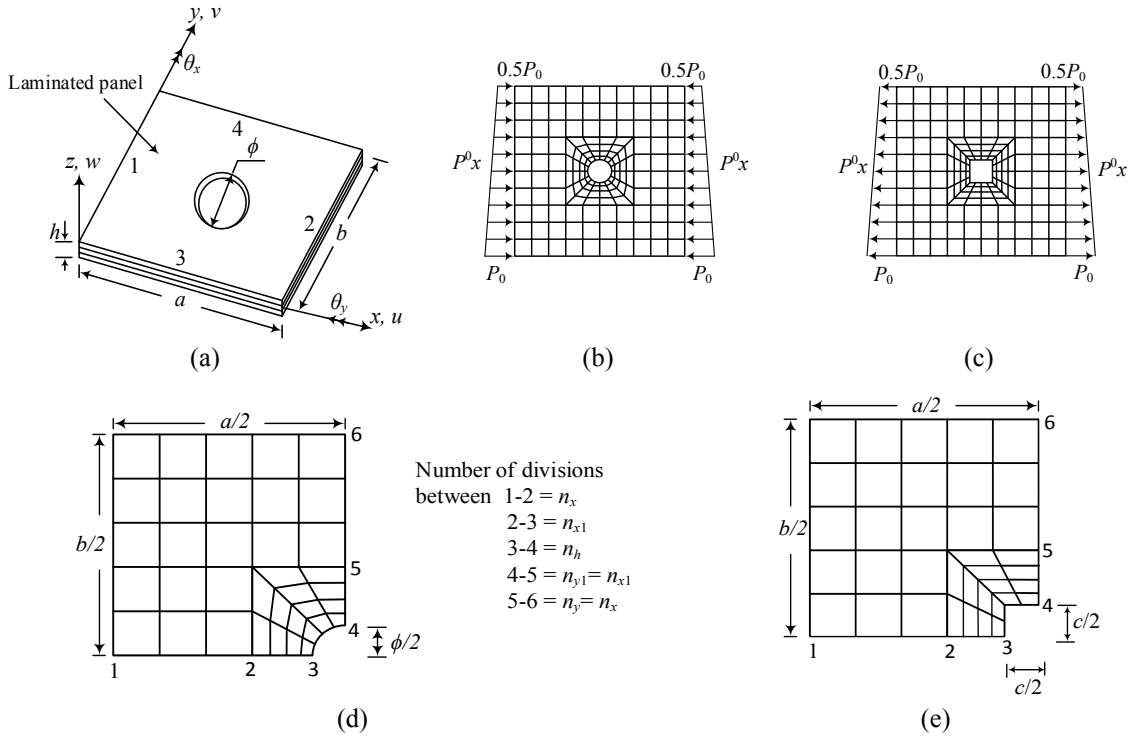

Fig. 1 (a) Geometry of the panel; (b) Mesh pattern over a full panel with circular cutout subjected to a typical in-plane load, $P_x^0 = P_0(1 - \alpha y/b)$, $\alpha = 0.5$; (c) Mesh pattern for a square cutout panel with a typical tensile edge load, $\alpha = 0.5$; (d) Detailed mesh pattern over a quarter panel of circular cutout; (e) Detailed mesh pattern over a quarter panel of square cutout

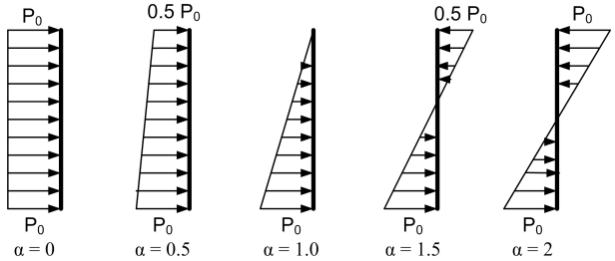

Fig. 2 Examples of linearly varying edge loads

2.1 Governing equations

The governing differential equation of motion for a discretized structure can be written in matrix form considering either tension or compression in-plane edge loads (Kumar *et al*. 2005)

$$[M]\{\ddot{q}\} + \left[[K] \pm P_0[K_G]\right]\{q\} = \{0\} \tag{1}$$

where $[K]$, $[K_G]$ and $[M]$ are assembled system stiffness, geometric stiffness and mass matrices

respectively. Here, $\{q\}$ represents the eigenvector for different modes of vibration/buckling.

The governing equations for the buckling and vibration problems can be obtained by reducing Eq. (1) as follows:

Static buckling problem:

When $\{\ddot{q}\} = 0$, Eq. (1) reduces to a static case as

$$[K]\{q\} \pm P_{cr}[K_G]\{q\} = \{0\} \tag{2}$$

Vibration problem:

When the plate vibrates harmonically under the action of in-plane compression or tension edge loads, Eq. (1) reduces to

$$[K]\{q\} \pm P_0[K_G]\{q\} - \omega^2[M]\{q\} = \{0\}. \tag{3}$$

In the above Eq. (3), if P_0 is equal to zero, then the equation represents a free vibration problem without in-plane load. If the in-plane load exists, then for a particular value of P_0, the square of the frequency (ω^2) becomes zero and then the corresponding load represents the critical buckling load.

2.2 Finite element formulation

In this study, a 9-node heterosis plate element is employed with five degrees of freedom (DOF) u, v, w, θ_x, and θ_y at all edge nodes and four DOF such as u, v, θ_x, and θ_y at the interior node. In order to develop heterosis element, the serendipity shape functions are used for transverse displacement w, and Lagrange shape functions for remaining DOF that includes u, v, θ_x, and θ_y as shown in Fig. 3. This type of element exhibits improved characteristics as compared to 8-node serendipity and 9-node Lagrange elements and offer higher accuracy for extremely thin plate configuration (Butalia *et al*. 1990, Hughes and Cohen 1978).

The present analysis is based on the Reissner-Mindlin hypothesis, which includes the effect of shear deformation in the formulation. As per this hypothesis, the mid-surface normal remains straight before and after bending but does not remain perpendicular to the mid-plane after bending.

The displacement field at any arbitrary distance z from the mid-plane can be expressed as (Kumar *et al*. 2005)

$$\begin{aligned} u(x,y,z) &= u_0(x,y) + z\theta_x(x,y) \\ v(x,y,z) &= v_0(x,y) + z\theta_y(x,y) \\ w(x,y,z) &= w_0(x,y) \end{aligned} \tag{4}$$

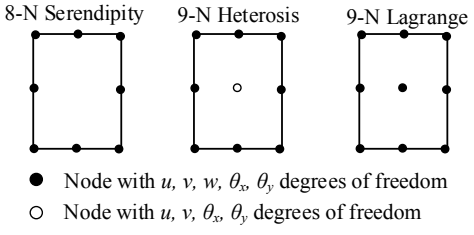

Fig. 3 Different types of plate elements

where u, v, and w are the displacement components at any point of panel space in the x-, y-, and z-directions; u_0, v_0, and w_0 describe the displacements of an arbitrary point (x, y) on the middle plane; The parameters θ_x and θ_y are rotations of the transverse normal cross-section in the xz and yz planes respectively.

The constitutive relation for the laminated panel is given by (Reddy 1996)

$$\{N\} = [C]\{\varepsilon\} \tag{5}$$

where $\{N\} = [N_x, N_y, N_{xy}, M_x, M_y, M_{xy}, Q_{xz}, Q_{yz}]^T$ represents the in-plane stress resultants (N), out of plane bending moments (M) and shear stress resultants (Q). Here, [C] is the constitutive matrix of the laminate (Reddy 1996). In order to compensate for the parabolic shear stress variation across the thickness of plate, a correction factor of 5/6 is used in the shear-shear coupling components of the constitutive matrix (Lal and Saini 2013). Using Green-Lagrange's strain-displacement expression (Bathe 1996), the linear strain-displacement matrix [B] and the non-linear strain-displacement matrix [B_G] have been worked out.

The different participating element level matrices such as elastic stiffness matrix [k_e], geometric stiffness matrix [k_G] and consistent mass matrix [m_e] have been derived using the corresponding energy expressions (Bathe 1996)

$$[k_e] = \int_{-1}^{+1}\int_{-1}^{+1} [B]^T [C][B]|J|\,d\xi\,d\eta \tag{6}$$

$$[k_G] = \int_{-1}^{+1}\int_{-1}^{+1} [B_G]^T [S][B_G]|J|\,d\xi\,d\eta \tag{7}$$

$$[m_e] = \int_{-1}^{+1}\int_{-1}^{+1} [\bar{N}]^T [I][\bar{N}]|J|\,d\xi\,d\eta \tag{8}$$

in which, $[\bar{N}]$ is the shape function matrix and [I] is the inertia matrix consisting of I_1, I_2 and I_3 which are given by $(I_1, I_2, I_3) = \sum_{k=1}^{L} \int_{z_{k-1}}^{z_k} \rho_k (1, z, z^2) dz$.

A computer code is developed using FORTRAN language to perform all the necessary computations. The global matrices are generated by assembling the corresponding element matrices and these assembled matrices are stored using skyline technique. The subspace iteration technique is adopted to solve the eigenvalue problems (Bathe 1996). In the code, selective integration scheme is incorporated for the generation of element elastic stiffness matrix. The 3 × 3 Gauss quadrature rule is adopted for membrane as well as bending terms, and 2 × 2 Gauss rule for shear terms to avoid possible shear locking. The geometric stiffness matrix is essentially a function of the in-plane stress distribution in an element due to applied edge loads. Since the stress field is non-uniform in nature for a given boundary and loading conditions, the plane stress analysis is carried out using standard FE procedure to determine the stresses at 3 × 3 Gauss sampling points. Accordingly, the integration for the generation of geometric stiffness matrix is done using 3 × 3 Gauss quadrature rule. The in-plane, transverse and rotary inertias are considered in the formulation of consistent mass matrix. This matrix has been evaluated using 3 × 3 Gauss rule.

3. Results and discussions

The problem considered here consists of a thin rectangular laminated panel (h/b = 0.01) with material constants, E_{11} = 25, E_{22} = 1.0, G_{12} = G_{13} = 0.50, G_{23} = 0.20 and v_{12} = 0.25 unless otherwise stated. In order to define the boundary conditions, the notations, *S* (simply supported), *C* (clamped) and *F* (free) are used in the string of various boundary conditions. For simplicity, the abbreviation *SSCC* in which, the first two successive alphabets indicate simply supported condition on x = 0 and x = a and the remaining two alphabets indicate clamped condition on y = 0 and y = b respectively in the order of edge numbers as shown in Fig. 1(a). In the analysis, the buckling results are calculated in two different stages. First, the pre-buckling analysis is carried out in order to determine the in-plane stress distribution within the plate element. The critical buckling loads are then calculated using the pre-buckling stresses.

The displacement boundary conditions considered for both pre-buckling and buckling analyses are as follows:

(1) Simply supported condition (*SSSS*):
- for pre-buckling stress analysis:
  $w = \theta_y = 0$ at x = 0, a; $w = \theta_x = 0$ at y = 0, b and u = 0, v = 0
  at two nodes along the edges $x = a/2$ and $y = b/2$ repectively.
- for buckling analysis:
  $u = w = \theta_y = 0$ along x = 0, a; $v = w = \theta_x = 0$ along y = 0, b.

(2) Clamped condition (*CCCC*):
- for pre-buckling stress analysis:
  $w = \theta_x = \theta_y = 0$ along x = 0, a and y = 0, b and u = 0, v = 0 at two nodes along the edges $x = a/2$ and $y = b/2$ respectively.
- for buckling analysis:
  $u = v = w = \theta_x = \theta_y = 0$ along x = 0, a and y = 0, b.

(3) Free condition (*F*): no restraint for both pre-buckling and buckling analyses except u = 0, v = 0 at two nodes along the edges $x = a/2$ and $y = b/2$ respectively, in the pre-buckling analysis.

The vibration frequency and the critical loads are presented in non-dimensional form as follows (Reddy and Phan 1985, Zhong and Gu 2007)

Non-dimensional frequency

$$\overline{\omega} = \omega_{abs} b^2 \sqrt{\left(\frac{\rho}{E_{22} h^2}\right)} \tag{9}$$

Non-dimensional load

$$\gamma_{cr} = \frac{P_{cr} b^2}{E_{22} h^3} \tag{10}$$

where ω_{abs} and P_{cr} are the absolute frequencies and absolute critical loads respectively.

3.1 Convergence studies

In a finite element analysis, the convergence studies are necessary for identifying the mesh size in order to achieve the proper convergence of the results. The mesh control parameters, $n_x = n_y$, n_{x1}

Table 1 Convergence of buckling loads for a *SSSS* edged angle-ply $(+45°/-45°)_s$ square panel with a central circular cutout under the action of uniaxial sinusoidal compressive and tensile edge loads

Cutout ratio (ϕ/b)	Mesh order for a full panel			No. of elements	Compressive buckling loads (γ_{cr})		Tensile buckling loads (γ_{cr})
	$n_x = n_y$	$n_{x1} = n_{y1}$	n_h				
0.3	2	1	24	88	37.169	(37.512)	222.232
	2	2	24	112	37.340	(37.352)	225.744
	2	3	24	136	37.363	(37.368)	224.678
	2	4	24	160	37.345	(37.326)	223.445
	2	5	24	184	37.346	(37.325)	222.523
	2	6	24	208	37.345	(37.321)	222.362
	2	7	24	232	34.669	(34.461)	222.295
	2	8	24	256	22.876	(22.537)	222.290
0.5	1	1	32	68	30.189	(31.216)	97.981
	1	2	32	100	30.641	(30.664)	98.370
	1	3	32	132	30.685	(30.679)	97.539
	1	4	32	164	30.669	(30.658)	97.059
	1	5	32	196	30.668	(30.657)	96.843
	1	6	32	228	30.667	(30.656)	96.789
	1	7	32	260	30.643	(30.621)	96.783

$= n_{y1}$ and n_h are given in Fig. 1(d) or (e). For a typical case of *SSSS* edged panel under the action of uniaxial compressive as well as tensile sinusoidal edge loading, the convergence studies have been carried out by varying the mesh control parameters. For cutout ratios of ϕ/b = 0.3 and 0.5, the buckling loads are evaluated and the results are presented in Table 1 for different mesh sizes. It is observed from the convergence results that around 160 elements are sufficient for fairly good results in the case of ϕ/b = 0.3, and around 164 elements for ϕ/b = 0.5 when the load is compressive in nature. However, when the load is tensile in nature, around 232 and 228 elements are sufficient for fairly good results in the cases of ϕ/b = 0.3 and 0.5 respectively. It is important to note that the number of elements required to achieve good convergence for tensile loading cases is comparatively more than that required for compressive type of loading. Further, the results are also extracted by using S8R5 shell element in ABAQUS and the results generated are given in parenthesis in Table 1. Finally, it is concluded that the convergence criterion has been satisfied for each type of problem considered in this paper.

3.2 Comparison with previous work– panel without cutout

Comparison studies are necessary for ascertaining the accuracy and efficiency of various matrices involved in the analysis of vibration and buckling problems. For validating the accuracy of stiffness and mass matrices, free vibration response of a square laminated panel without cutout is carried out by using 9-node heterosis element (9-NHE), 9-node Lagrange element (9-NLE) and 8-node serendipity element (8-NSE) along with the closed-form solutions (CFS) of Reddy and Phan (1985) as shown in Table 2. Similarly, to ascertain the accuracy of geometric stiffness matrix, the buckling analysis of cross-ply square laminate under the application of different types of non

Table 2 Non-dimensionalised frequency of angle-ply laminated simply supported unstiffened square plate; $E_{11}/E_{22} = 40$, $G_{12} = G_{13} = 0.6E_{22}$, $G_{23} = 0.5E_{22}$, $\upsilon_{12} = 0.25$

	2 layers (45/-45)			CFS (Reddy and Phan 1985)	8 layers (45/-45/45…)			CFS (Reddy and Phan 1985)
b/*h*	Present results				Present results			
	9-NHE	9-NLE	8-NSE		9-NHE	9-NLE	8-NSE	
5	10.335	10.244	10.243	10.335	12.892	12.863	12.862	12.892
10	13.044	12.975	12.975	13.044	19.289	19.235	19.235	19.289
20	14.179	14.154	14.153	14.179	23.259	23.225	23.225	23.259
25	14.338	14.322	14.321	14.338	23.924	23.899	23.899	23.924
50	14.561	14.557	14.556	14.561	24.909	24.902	24.901	24.909
100	14.618	14.617	14.617	14.618	25.176	25.174	25.174	25.176

Table 3 Comparison of buckling loads for a cross-ply square panel (0/90/0) under linearly varying loads; $E_{11}/E_{22} = 40$, $G_{12} = G_{13} = 0.6E_{22}$, $G_{23} = 0.5E_{22}$ and $\upsilon_{12} = 0.25$

Loading pattern (α)	Source	$h/b = 0.01$	$h/b = 0.05$	$h/b = 0.1$
0.5	CFS (Zhong and Gu 2007)	47.267	41.075	29.432
	9 – HPE	47.261	40.939	29.228
	9 – LPE	47.259	40.930	29.225
	8 – SPE	47.256	40.921	29.120
1.0	CFS (Zhong and Gu 2007)	64.982	56.705	40.999
	9 – HPE	64.975	56.486	40.525
	9 – LPE	64.962	56.478	40.514
	8 – SPE	64.960	56.457	40.500
1.5	CFS (Zhong and Gu 2007)	91.374	80.336	47.708
	9 – HPE	91.355	79.989	48.300
	9 – LPE	91.338	79.957	48.291
	8 – SPE	91.331	79.930	48.285
2.0	CFS (Zhong and Gu 2007)	129.785	114.837	47.872
	9 – HPE	129.758	114.167	48.720
	9 – LPE	129.730	114.152	48.660
	8 – SPE	129.725	113.980	48.514

uniform edge compressive loads have been carried out using same three kinds of elements for different *h*/*b* ratios and the results are tabulated in Table 3 along with the closed form solutions of Zhong and Gu (2007). It can be observed that though all the elements give satisfactory results both in the cases of vibration and buckling analyses, better accuracy has been exhibited by the heterosis element, and hence, the same element has been used in the rest of the work.

3.3 Comparison study – panel with cutout

The comparative study of panel with different sized circular cutout is further extended to

Table 4 Comparison of buckling loads for a *SSSS* edged square laminated panel with circular cutouts under uniform edge load; E_{11} = 130.0 GPa, E_{22} = 10.0 GPa, $G_{12} = G_{13}$ = 5.0 GPa, G_{23} = 3.4 GPa, and v_{12} = 0.35

ϕ/b	40 layers $(45/-45/0/90)_{5S}$, b/h = 75		8 layers $(0/90)_{2S}$, b/h = 100	
	Present	Jain and Kumar (2004)	Present	Ghannadpour *et al*. (2006)
0.0	19.16 (19.14)	19.23	13.82 (13.81)	13.79
0.1	18.41 (18.42)	18.56	12.83 (12.83)	12.80
0.2	16.94 (16.97)	17.10	10.84 (10.85)	10.82
0.3	15.40 (15.42)	15.30	8.98 (8.97)	8.97
0.4	14.63 (14.63)	14.63	7.52 (7.51)	7.51
0.5	13.96 (13.97)	13.84	6.40 (6.39)	6.39

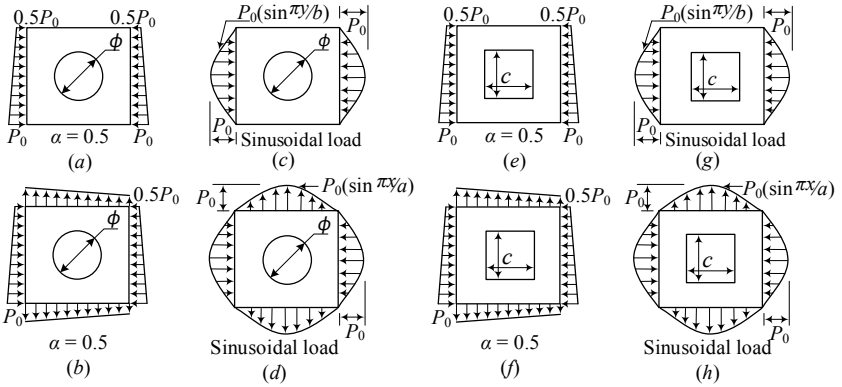

Fig. 4 Square panels under various kinds of uniaxial and biaxial non-uniform edge loading

ascertain the buckling behavior of square laminated panel under uniformly distributed edge load. The effect of 8-layered $(0/90)_{2s}$ and 40-layered $(45/-45/0/90)_{5s}$ laminated panels have been studied under different cutout sizes by using heterosis element. The results are tabulated in Table 4 along with the results obtained using S8R5 element in ABAQUS, and results of similar studies carried by other researchers and reported in the literature (Jain and Kumar 2004, Ghannadpour *et al*. 2006). The ABAQUS results are shown within the parenthesis. The good agreement is found between the present study and those from the literature and FE package–ABAQUS.

3.4 Buckling and vibration results under compressive and tensile edge loading

In this section, the vibration and buckling behavior of four layered symmetric laminated panels are examined by considering various parameters such as ply-orientation, edge condition, load type, panel aspect ratio and cutout size. The typical loading cases considered in the present investigation as shown in Fig. 4. The uniaxial loading case shown here is compressive in nature. Therefore, the corresponding uniaxial tensile loading case can be obtained by reserving the loading direction.

3.4.1 Buckling of laminated panels under the action of uniaxial varying edge load

The effect of different ply-orientations on the buckling behavior of four layered symmetric $(\pm\theta^{\circ})_s$ laminated panel subjected to uniaxial varying compressive edge load (α = 0.5) has been

studied for the panels with circular and square cutouts.

Fig. 5(a) shows the variation of buckling loads with ply-orientations for different sized circular cutouts (ϕ/b = 0 to 0.7). It can be seen from the figure that for any given cutout ratio ϕ/b, the buckling load parameter γ_{cr} gradually increases with the increased ply-orientation till it reaches a maximum at certain ply-angle beyond which, it reduces with further increase of the ply-orientation. The maximum buckling load γ_{cr} occurs at $\theta \approx (\pm 45°)_s$ and shift towards $\theta \approx (\pm 60°)_s$, as the ϕ/b increases. It is also seen that for $\theta = (\pm 0°)_s$ to around $(\pm 55°)_s$, the value of γ_{cr} predominantly reduces with the increased ϕ/b. Beyond $\theta = (\pm 55°)_s$, the variation of γ_{cr} with ϕ/b is insignificant.

Similar studies have been carried out for the same panel with square cutout (c/b = 0 to 0.7) and the results are depicted in Fig. 5(b). One can observe from the figures that the buckling characteristic of square cutout panel is almost similar to that of circular cutout panel without much change in the values of γ_{cr}.

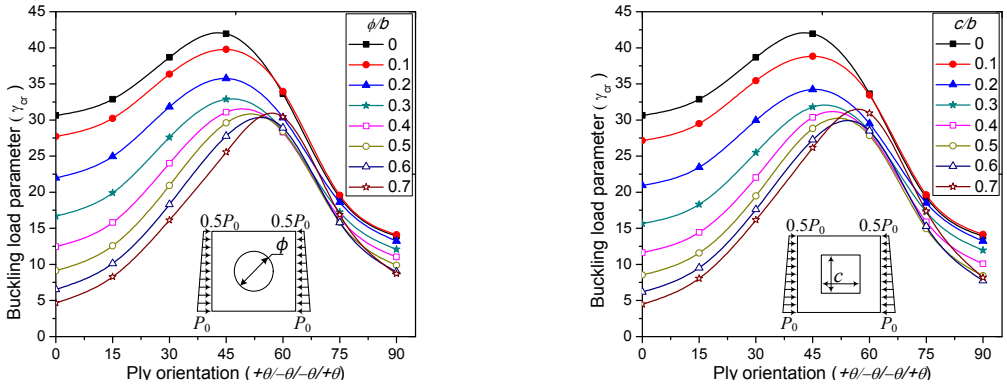

(a) (b)

Fig. 5 Compressive buckling variation of different ply-oriented *SSSS* edged square panels with different ratios of (a) circular cutouts; and (b) square cutouts under the action of uniaxial varying load for $\alpha = 0.5$

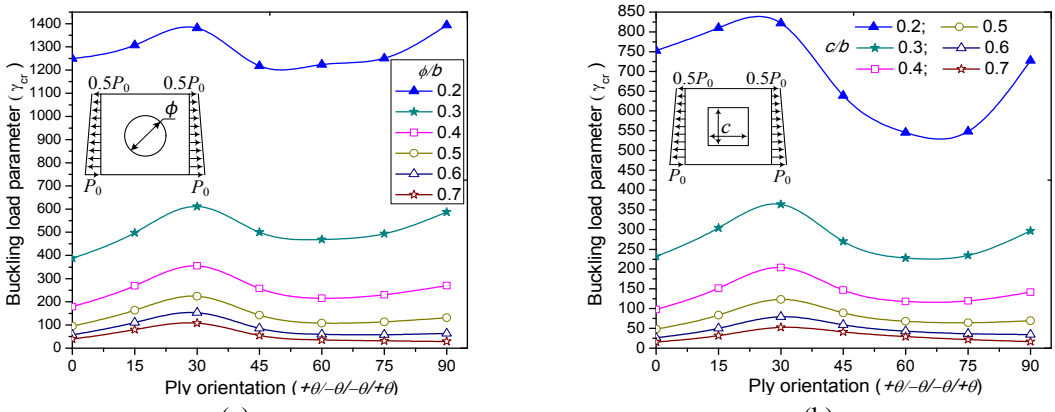

(a) (b)

Fig. 6 Tensile buckling variation of different ply-oriented *SSSS* edged square panels with different ratios of (a) circular cutouts; and (b) square cutouts under the action of uniaxial varying load for $\alpha = 0.5$

For the same problem, the buckling behavior of the panel with circular and square cutouts is examined by applying tensile varying edge load ($\alpha = 0.5$) and the results are shown in Figs. 6(a)-(b) respectively. It is observed from Figs. 6(a)-(b) that for any given ply-orientation, the tensile buckling load γ_{cr} continuously decreases with the increase of cutout ratio (ϕ/b or c/b). But, for any given ply-angle, the variation of buckling resistance with the increase of cutout ratio is significant as the ϕ/b or c/b approaches a value of 0.4 and there onwards, it is almost insignificant. It may be attributed towards the fact that the tensile stresses are comparatively more pronounced at lower ϕ/b or c/b ratios. It is also observed from the figures that the value of γ_{cr} is found to be higher at $\theta = (\pm 30°)_s$ and $(\pm 90°)_s$ for ϕ/b or c/b (≤ 0.4). But, for higher ϕ/b or c/b (≥ 0.5), the value of γ_{cr} is generally found to be higher only at $\theta = (\pm 30°)_s$. Further, it is worth to mention that although the buckling behavior is similar for both circular and square cutout panels, quite higher buckling

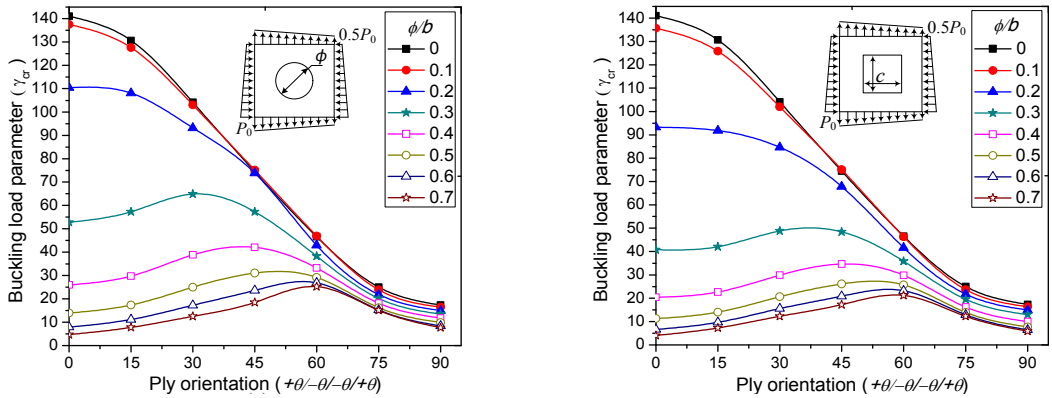

Fig. 7 Variation of buckling parameter γ_{cr} for different ply-oriented *SSSS* edged square panels with different ratios of (a) circular cutouts; and (b) square cutouts under the action of biaxial varying load $\alpha = 0.5$

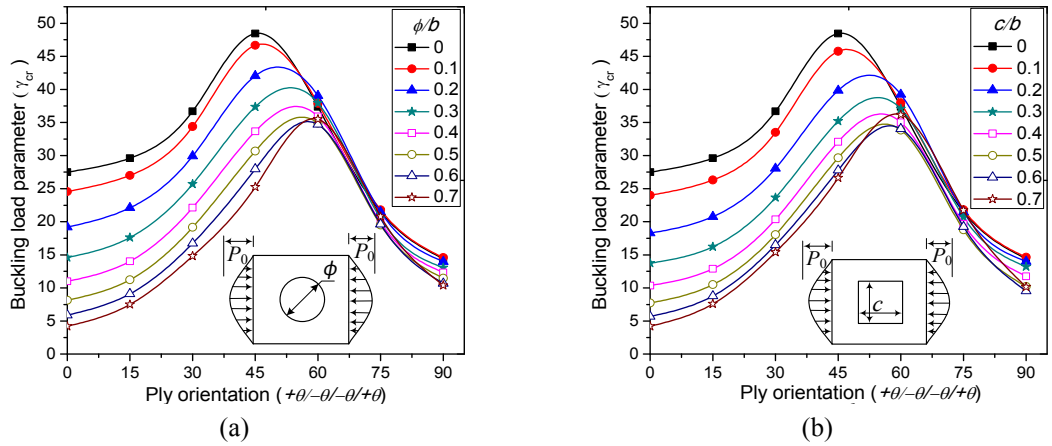

Fig. 8 Variation of compressive buckling parameters γ_{cr} for different ply-oriented *SSSS* edged square panels with different ratios of (a) circular cutouts; and (b) square cutouts under uniaxial sinusoidal load

resistance is observed in circular cutout panels as compared to that of square cutout panels.

The effect of biaxial (compression-tension) type of edge load ($\alpha = 0.5$) on buckling behavior of different ply-oriented panel with circular and square cutouts have been studied and the results are illustrated in Figs. 7(a)-(b) respectively. It is observed from the figures that for any given ply-orientation, the value of γ_{cr} continuously reduces with the increased cutout ratios (ϕ/b or c/b). The decrease in γ_{cr} with increased cutout ratio is significant at $\theta = (\pm 0°)_s$ and insignificant at $\theta \geq (\pm 60°)_s$. It is also observed from the figures that for lower ϕ/b or c/b (≤ 0.2), the γ_{cr} is found to be maximum at $\theta = (\pm 0°)_s$ and thereafter decreases with a further increased ply-orientation. However, for the cutout ratio (ϕ/b or $c/b \geq 0.3$), the value of γ_{cr} gradually increases with the increased ply-orientation till it reaches a maximum at certain ply-angle and then, starts reducing with a further increase in ply-angles. However, the buckling values of square cutout panels are found to be almost equal with that of circular cutout panels for any given cutout ratio and ply-orientation.

3.4.2 Buckling behavior of laminated panels subjected to sinusoidal edge loading

The variation of γ_{cr} with the ply-angles $(\pm\theta°)_s$ for *SSSS* edged panels with circular and square cutouts subjected to uniaxial compressive sinusoidal edge load is shown in Figs. 8(a)-(b) respectively. It is noticed from the figures that the buckling behavior is almost similar to the load case ($\alpha = 0.5$) shown in Figs. 5(a)-(b) without much difference in the values of γ_{cr}. However, the role of ϕ/b or c/b on γ_{cr} is predominant in the ply-orientation range of $(\pm 0°)_s \leq \theta < (\pm 60°)_s$. But, for $\theta \geq (\pm 60°)_s$, the effect of ϕ/b or c/b on γ_{cr} is negligible. It can also be observed that the values of γ_{cr} are almost same for both types of cutouts for any given cutout ratio and ply-orientation.

Similar studies have been carried out for the same circular and square cutout panels subjected to uniaxial tensile sinusoidal edge load and the results are depicted in Figs. 9(a)-(b) respectively. The tensile buckling behavior of the panels shown in Figs. 9(a)-(b) is almost similar to the load case ($\alpha = 0.5$) shown in Figs. 6(a)-(b) irrespective of cutout ratios except for ϕ/b or $c/b = 0.2$. It is to be noted that the panel under the load case ($\alpha = 0.5$) shows higher buckling resistance as compared to that of the panel under sinusoidal edge load irrespective of ply-orientation as well as cutout ratios. It may be due to the fact that in the case of sinusoidal load, the compressive stress field is more pronounced in the central region of the panel as compared to that of tensile load case

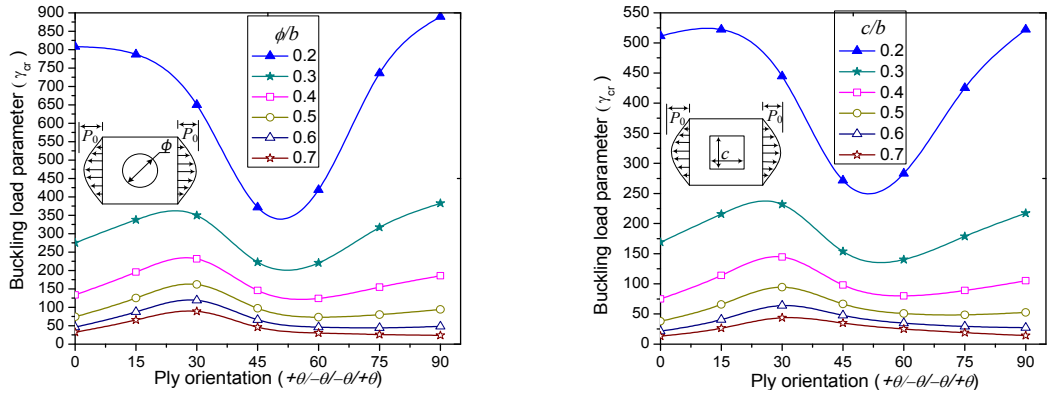

Fig. 9 Variation of tensile buckling parameters γ_{cr} for different ply-oriented *SSSS* edged square panels with different ratios of (a) circular cutouts; and (b) square cutouts under uniaxial sinusoidal load

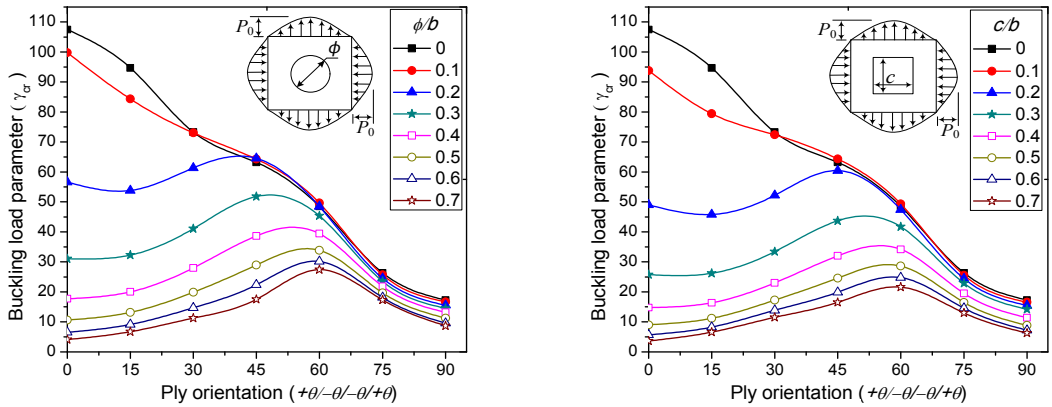

Fig. 10 Buckling variation of different ply-oriented *SSSS* edged square panels with different ratios of (a) circular cutouts; and (b) square cutouts under biaxial sinusoidal load

at $\alpha = 0.5$. However, in this case, higher values of γ_{cr} have been observed for the ply-orientations of $(\pm 0°)_s$ and $(\pm 90°)_2$ only for ϕ/b or $c/b = 0.2$ whereas, for the remaining cutout ratios (> 0.2), the value of γ_{cr} is found to be maximum at $\theta = (\pm 30°)_s$. Furthermore, the circular cutout panel shows more tensile buckling resistance as compared to that of square cutout panel for all ply-orientations.

The effect of biaxial sinusoidal (compression-tension) edge load on buckling behavior of different ply-oriented *SSSS* edged square panels with circular and square cutouts have been studied and the results are depicted in Figs. 10(a)-(b) respectively. It is observed from Figs. 10(a)-(b) that the value of γ_{cr} continuously decreases with the increase of $(\pm\theta°)_s$ for the cases of ϕ/b or $c/b \leq 0.1$. However, for the cases of ϕ/b or $c/b > 0.1$, the buckling load initially increases with the increase in ply-orientation and reaches a maximum value at certain ply-angle and thereafter starts decreasing to a minimum with the further increase of $(\pm\theta°)_s$. The ply-orientation $(\pm\theta°)_s$ at which γ_{cr} is maximum shifts from $(\pm 45°)_s$ to $(\pm 60°)_s$ as ϕ/b or c/b varies from 0.2 to 0.7.

From the above study, it may be concluded that if there is, at least, one pair of in-plane compressive edge load, then there will not be any significant change in the values of γ_{cr} for both circular and square cutout panels.

3.4.3 Effect of boundary conditions along with cutout sizes

The effect of degree of edge restraints on buckling behavior of a typical layered panel with $\theta = (\pm 75°)_s$ is examined by considering fourteen different types of boundary conditions and the results are illustrated in Figs. 11(a)-(b). It is observed from Fig. 11(a) that γ_{cr} generally increases with increase in the degree of edge restraints for any given ϕ/b. In the cases of *CCCC*, *CSCC*, and *SSCC* edge conditions, the value of γ_{cr} initially decreases with the increased cutout ratios up to $\phi/b = 0.2$ and then increases with a further increase of ϕ/b. Similarly, for *CSCS*, *CCSS*, *CSSC*, *SCSS*, and *SSSS* boundary conditions, the value of γ_{cr} also decreases up to $\phi/b = 0.5$ and marginally increases beyond this cutout ratio. This may be attributed to the load path being redirected from the vicinity of cutout towards the stiffer region (Soni *et al.* 2013). However, for other edge conditions, the value of γ_{cr} continuously reduces with the increase of ϕ/b.

Similar kind of behavior is also observed when the same panel is subjected to biaxial sinusoidal edge load except *CCCC*, *CSCC*, and *SSCC* boundary conditions as can be seen in Fig. 11(b).

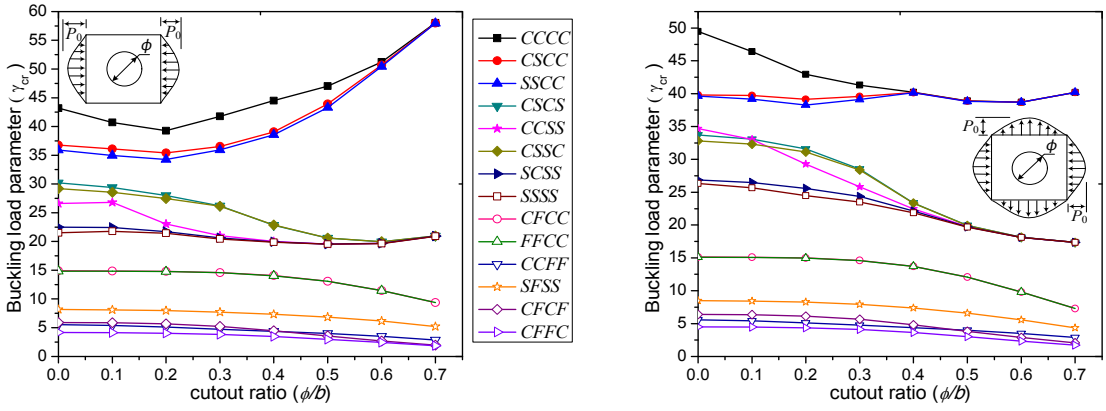

Fig. 11 Effect of cutout ratios ϕ/b and boundary conditions on variation of γ_{cr} for $(\pm 75°)_s$ layup square panel subjected to (a) uniaxial sinusoidal compressive load; and (b) biaxial sinusoidal compressive-tensile load

Further, it is also observed that the value of γ_{cr} remains same for any given size of cutout in both the cases of uniaxial and biaxial loadings, if at least, one edge of the panel is free.

3.4.4 Effect of panel aspect ratios along with size of cutouts

The combined effects of panel aspect ratios a/b and cutout ratios ϕ/b on the buckling behavior of $(\pm 45°)_s$ ply-oriented *SSSS* edged panel subjected to compressive and tensile type of sinusoidal edge loads have been studied and the results are illustrated in Figs. 12(a)-(b) respectively. The panel aspect ratios, a/b = 1.0, 1.6, 2.0, 2.6 and 3.0 along with ϕ/b = 0.3 to 0.7 are considered in this section. The different panel aspect ratio is obtained by varying the length of panel, a and keeping its width, b constant. It can be observed from Fig. 12(a) that the value of compressive buckling

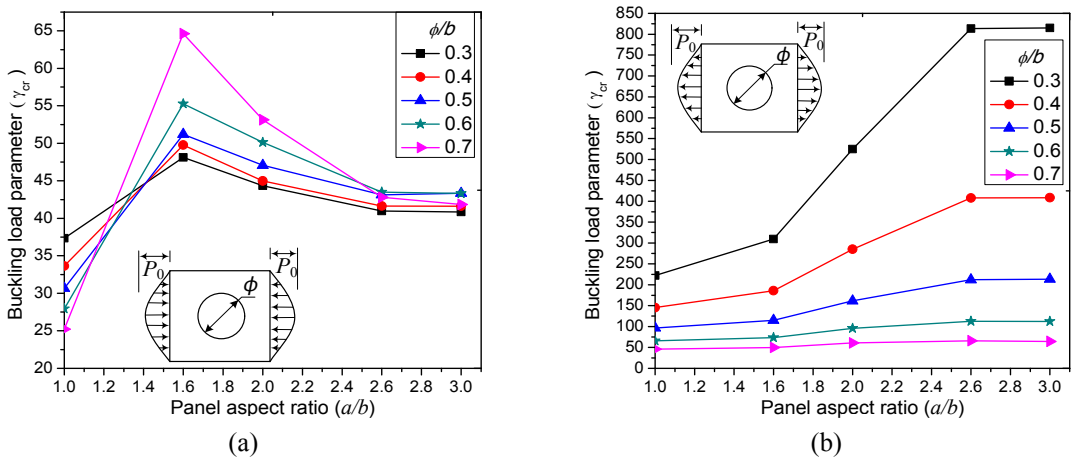

Fig. 12 Variation of γ_{cr} for different aspect ratios of $(\pm 45°)_s$ ply-oriented *SSSS* edged panels with various sized cutouts under the application of (a) compressive sinusoidal load; and (b) tensile sinusoidal load

load decreases with the increase in ϕ/b ratio in the case of square panel. The trend is found to be reversed for panels with higher aspect ratios. However, the values of γ_{cr} are found to be maximum for the panel aspect ratio equal to 1.6.

A different behavior is observed when the same panel is subjected to tensile type of sinusoidal edge load as shown in Fig. 12(b). It is observed from the figure that the tensile buckling load γ_{cr} decreases with an increase in ϕ/b for all aspect ratios of the panel. It is also noticed that for any given ϕ/b, the buckling resistance of the panel continuously increases with an increase in panel aspect ratio a/b and is found to be maximum at $a/b = 2.6$. Further, the value of γ_{cr} remains almost constant with an increase of a/b. This may be due to the fact that the tensile buckling is a local buckling phenomenon due to localized compressive stress around the cutout, which remains same for all higher aspect ratios. It is worth to mention that as the ϕ/b ratio reaches 0.7, the effect of panel aspect ratio is almost negligible and it remains almost constant.

3.4.5 Vibration characteristics of laminated panel with cutout

The free vibration behavior of a $(\pm 45°)_s$ ply-oriented panel with centrally placed circular cutouts under the action of compressive and tensile types of sinusoidal edge loads have been studied and the results are illustrated in Figs. 13(a)-(b) respectively. It is observed from Fig. 13(a) that the frequency at zero load gives the fundamental frequency, and this frequency increases with the increase in ϕ/b and is found to be maximum at $\phi/b = 0.7$. It may be attributed to the decrease of panel stiffness with the increased cutout size. However, for any given ϕ/b, as the intensity of compressive load increases, the frequency of oscillation decreases and reduces to zero at the onset of buckling.

It is observed from Fig. 13(b) that for any given cutout ratio ϕ/b, the frequency of oscillation initially increases with the increase of in-plane edge load. As the load further increases, the frequency starts decreasing and becomes zero at the onset of tensile buckling. The rate of increase of frequency is significant at lower cutout ratios and found to be maximum at $\phi/b = 0.2$ and minimum at $\phi/b = 0.7$. It may be due to the dominance in the tensile stresses as compared with that of compressive stresses at lower ϕ/b, and this dominance in tensile stresses gradually reduces as the cutout size increases.

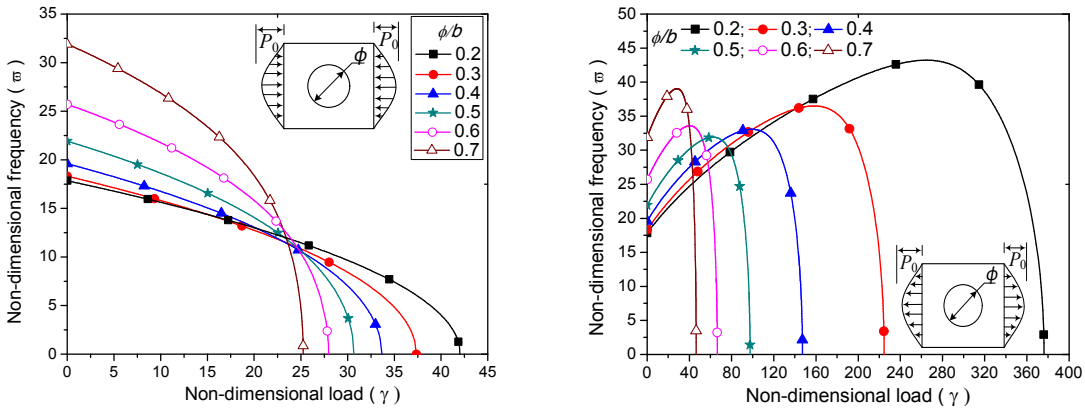

Fig. 13 Variation of frequency parameters (ϖ) for different cutout ratios of $(\pm 45°)_s$ ply-oriented square panel under (a) uniaxial compressive sinusoidal load; (b) uniaxial tensile sinusoidal load

4. Conclusions

The results from the studies of the tensile and compressive buckling and vibration characteristics of composite laminated panel with circular and square cutouts subjected to non-uniform in-plane edge loading and can be summarized as follows:

(1) The natural frequency is found to decrease with the increase in compressive load and reduces to zero when the in-plane load approaches the critical buckling load. In case of tensile edge load, the frequency of oscillation initially increases with the increase in applied edge load up to certain extent and thereafter decreases with the further increase in load and reduces to zero at the onset of tensile buckling.
(2) The type of loading and ply-orientation play a significant role in the buckling behavior of a panel with and without cutout. However, the maximum buckling resistance of ply-angle range is evaluated for each type of loading case and cutout ratios.
(3) For any given ply-angle, the buckling load continuously decreases with the increased cutout size when the panel is subjected to uniaxial tensile or biaxial (compressive-tensile) loading cases. This is also true for uniaxial compressive loading cases except for some particular ply-orientations with higher sized cutouts, for which, an increase in the buckling load is observed.
(4) The tensile buckling loads are found to be significantly lesser at higher sized cutouts as compared to that of lower sized cutouts irrespective of ply-orientations.
(5) The circular and square cutouts show similar buckling behavior without much change in the value of buckling loads for both uniaxial compressive and biaxial (compressive-tensile) loading cases. But, in the case of uniaxial tensile edge load, circular cutout panel shows comparatively higher buckling load as compared to that of panel with square cutout.
(6) In the cases of uniaxial compressive and biaxial (compressive-tensile) edge loads, the presence of smaller sized cutout (≤ 0.1) may be neglected due to their insignificant change in the value of buckling loads.
(7) The buckling load of perforated panel is highly influenced by panel aspect ratios. In case of square panel, the compressive buckling load generally decreases with the increase in cutout sizes. The trend is reversed for higher panel aspect ratios. Maximum compressive buckling load is observed as the panel aspect ratio approach 1.6. In case of tensile edge load, the tensile buckling load continuously decreases with the increase in the cutout ratio. However, for any given cutout ratio, the buckling load increases with the increased panel aspect ratio and is found to be maximum at $a/b = 2.6$ and thereafter, it almost remains constant with the further increase in a/b.
(8) The critical buckling load increases with the increase in the degree of edge restraints. In some particular cases, the buckling load initially decreases with the increase in cutout size up to a certain stage and thereafter increases with a further increase in the cutout size.

Acknowledgments

Valuable suggestions from Prof. H.B. Nagaraj, Prof. P. Prasanna Kumar and Prof. Sutapa Hazra, B.M.S. College of Engineering, Bengaluru are acknowledged with thanks.

References

Afsharmanesh, B., Ghaheri, A. and Taheri-Behrooz, F. (2014), "Buckling and vibration of laminated composite circular plate on winkler-type foundation", *Steel Compos. Struct., Int. J.*, **17**(1), 1-19.

Altunsaray, E. and Bayer, I. (2014), "Buckling of symmetrically laminated quasi-isotropic thin rectangular plates", *Steel Compos. Struct., Int. J.*, **17**(3), 305-320.

Ashour, A.S. (2003), "Buckling and vibration of symmetric laminated composite plates with edges elastically restrained", *Steel Compos. Struct., Int. J.*, **3**(6), 439-450.

Aydin Komur, M. and Sonmez, M. (2008), "Elastic buckling of rectangular plates under linearly varying in-plane normal load with a circular cutout", *Mech. Res. Commun.*, **35**(6), 361-371.

Baba, B.O. (2007), "Buckling behavior of laminated composite plates", *J. Reinf. Plast. Compos.*, **26**(16), 1637-1655.

Baba, B.O. and Baltaci, A. (2007), "Buckling characteristics of symmetrically and antisymmetrically laminated composite plates with central cutout", *Appl. Compos. Mater.*, **14**(4), 265-276.

Bathe, K.J. (1996), *Finite Element Procedures*, Prentice Hall, Englewood Cliffs, NJ, USA.

Butalia, T.S., Kant, T. and Dixit, V.D. (1990), "Performance of heterosis element for bending of skew rhombic plates", *Comput. Struct.*, **34**(1), 23-49.

Deolasi, P.J., Datta, P.K. and Prabhakar, D.L. (1995), "Buckling and vibration of rectangular plates subjected to partial edge loading (compression or tension)", *J. Struct. Eng.*, **22**(3), 135-144.

Ghannadpour, S.A.M., Najafi, A. and Mohammadi, B. (2006), "On the buckling behavior of cross-ply laminated composite plates due to circular/elliptical cutouts", *Compos. Struct.*, **75**(1), 3-6.

Hughes, T.J.R. and Cohen, M. (1978), "The "heterosis" finite element for plate bending", *Comput. Struct.*, **9**(5), 445-450.

Jain, P. and Kumar, A. (2004), "Postbuckling response of square laminates with a central circular/elliptical cutout", *Compos. Struct.*, **65**(2), 179-185.

Komur, M.A. and Sonmez, M. (2015), "Elastic buckling behavior of rectangular plates with holes subjected to partial edge loading", *J. Construct. Steel Res.*, **112**, 54-60.

Komur, M.A., Sen, F., Ataş, A. and Arslan, N. (2010), "Buckling analysis of laminated composite plates with an elliptical/circular cutout using FEM", *Adv. Eng. Software*, **41**(2), 161-164.

Kremer, T. and Schürmann, H. (2008), "Buckling of tension-loaded thin-walled composite plates with cut-outs", *Compos. Sci. Technol.*, **68**(1), 90-97.

Kumar, D. and Singh, S.B. (2010), "Effects of boundary conditions on buckling and postbuckling responses of composite laminate with various shaped cutouts", *Compos. Struct.*, **92**(3), 769-779.

Kumar, L.R., Datta, P.K. and Prabhakara, D.L. (2002), "Tension buckling and vibration behaviour of curved panels subjected to non-uniform in-plane edge loading", *Int. J. Struct. Stab. Dyn.*, **2**(3), 409-423.

Kumar, L.R., Datta, P.K. and Prabhakara, D.L. (2003), "Tension buckling and dynamic stability behaviour of laminated composite doubly curved panels subjected to partial edge loading", *Compos. Struct.*, **60**(2), 171-181.

Kumar, L.R., Datta, P.K. and Prabhakara, D.L. (2005), "Vibration and stability behavior of laminated composite curved panels with cutout under partial in-plane loads", *Int. J. Struct. Stab. Dyn.*, **5**(1), 75-94.

Kutlu, D. (2011), "Influence of aspect ratio and fibre orientation on the stability of simply supported orthotropic skew plates", *Steel Compos. Struct., Int. J.*, **11**(5), 359-374.

Lal, R. and Saini, R. (2013), "Buckling and vibration of non-homogeneous rectangular plates subjected to linearly varying in-plane force", *Shock Vib.*, **20**(5), 879-894.

Leissa, A.W. and Ayoub, E.F. (1988), "Vibration and buckling of a simply supported rectangular plate subjected to a pair of in-plane concentrated forces", *J. Sound Vib.*, **127**(1), 155-171.

Narayana, A.L., Rao, K. and Kumar, R.V. (2014), "Buckling analysis of rectangular composite plates with rectangular cutout subjected to linearly varying in-plane loading using fem", *Sadhana*, **39**(3), 583-596.

Reddy, J.N. (1996), *Mechanics of Laminated Composite Plates*, CRC press, New York, NY, USA.

Reddy, J.N. and Phan, N.D. (1985), "Stability and vibration of isotropic, orthotropic and laminated plates according to a higher-order shear deformation theory", *J. Sound Vib.*, **98**(2), 157-170.

Shimizu, S. (2007), "Tension buckling of plate having a hole", *Thin-Wall. Struct.*, **45**(10), 827-833.
Singh, S., Kulkarni, K., Pandey, R. and Singh, H. (2012), "Buckling analysis of thin rectangular plates with cutouts subjected to partial edge compression using FEM", *J. Eng. Des.*, **10**(1), 128-142.
Soni, G., Singh, R. and Mitra, M. (2013), "Buckling behavior of composite laminates (with and without cutouts) subjected to nonuniform in-plane loads", *Int. J. Struct. Stab. Dyn.*, **13**(8), 1350044 (20 p).
Srivastava, A., Datta, P. and Sheikh, A. (2003), "Buckling and vibration analysis of stiffened plate subjected to in-plane concentrated load", *Struct. Eng. Mech., Int. J.*, **15**(6), 685-704.
Tang, Y. and Wang, X. (2011), "Buckling of symmetrically laminated rectangular plates under parabolic edge compressions", *Int. J. Mech. Sci.*, **53**(2), 91-97.
Topal, U. and Uzman, Ü. (2008), "Maximization of buckling load of laminated composite plates with central circular holes using MFD method", *Struct. Multidisc. Optimiz.*, **35**(2), 131-139.
Walker, M. (1998), "Optimisation of symmetric laminates with internal line supports for maximum buckling load", *Struct. Eng. Mech., Int. J.*, **6**(6), 633-641.
Yazici, M., Ozcan, R., Ulku, S. and Okur, I. (2003), "Buckling of composite plates with U-shaped cutouts", *J. Compos. Mater.*, **37**(24), 2179-2195.
Zhong, H. and Gu, C. (2007), "Buckling of symmetrical cross-ply composite rectangular plates under a linearly varying in-plane load", *Compos. Struct.*, **80**(1), 42-48.

CC